Available online at www.sciencedirect.com
ScienceDirect
Developmental Biology 304 (2007) 90–101
DEVELOPMENTAL BIOLOGY
www.elsevier.com/locate/ydbio

Tissue-specific laminin expression facilitates integrin-dependent association of the embryonic wing disc with the trachea in *Drosophila*

Yoshiko Inoue [a], Shigeo Hayashi [a,b,*]

[a] *Riken Center for Developmental Biology, 2-2-3 Minatojima-minamimachi, Chuo-ku Kobe 650-0047, Japan*
[b] *Department of Life Science, Kobe University Graduate School of Science and Technology, Japan*

Received for publication 25 September 2006; revised 24 November 2006; accepted 10 December 2006
Available online 15 December 2006

Abstract

The interaction of heterologous tissues involves cell adhesion mediated by the extracellular matrix and its receptor integrins. The *Drosophila* wing disc is an ectodermal invagination that contacts specific tracheal branches at the basolateral cell surface. We show that an α subunit of laminin, encoded by *wing blister* (*wb*), is essential for the establishment of the interaction between the wing and trachea. During embryogenesis, wing disc cells present Wb at their basolateral surface and extend posteriorly, expanding their association to more posteriorly located tracheal branches. These migratory processes are impaired in the absence of the trachea, Wb, or integrins. Time-lapse and transmission electron microscopy analyses suggest that Wb facilitates integrin-dependent contact over a large surface and controls the cellular behavior of the wing cells, including their exploratory filopodial activity. Our data identify Wb laminin as an extracellular matrix ligand that is essential for integrin-dependent cellular migration in *Drosophila*.

Keywords: Cell adhesion; Cell migration; Wing disc; Trachea; Integrin; Extracellular matrix; Laminin

Introduction

Organs in the animal body are assemblages of multiple tissues with distinct cellular properties that function as units to execute specific behavioral or physiological tasks. The movement of tissues and their mutual recognition through cell–cell interactions facilitate the assembly of tissues of different developmental origins, which is essential for the proper shaping of organs and their correct positional placement in the body cavity.

Because the basal surfaces of tissues are usually covered by the basement membrane, which is composed of the extracellular matrix (ECM), associating tissues interact indirectly through the ECM. The ECM acts as a substrate for cell adhesion via the integrin family of receptors (Bökel and Brown, 2002). The integrins and their ligands in the ECM play key roles in development, immune responses, leukocyte trafficking, and cancer (Hynes, 2002). Cell–ECM adhesions connect the ECM to the intracellular cytoskeleton, transduce bidirectional signals between the extra- and intracellular compartments, and are suggested to be crucial for cell behavior (Sepulveda et al., 2005). Although the integrin–ECM interaction has been studied extensively in culture, progress in studying how guided migration is controlled by the ECM has been slow because it is difficult to reproduce the proper extracellular environment in vitro.

Our studies of the development of the wing imaginal disc in the *Drosophila* embryo have provided a new paradigm for heterologous tissue interactions and guided migration via the ECM. The development of the thoracic imaginal discs, including those for the wing, haltere, and three pairs of leg primordia, starts in stage 11 of embryogenesis. After the cells in the presumptive thoracic imaginal discs start to express the homeobox gene *Distal-less* (*Dll*) (Cohen, 1990), the primordia respond to decapentaplegic and epidermal growth factor receptor signals to acquire either a dorsal (wing) or ventral (leg) disc fate in the mesothoracic segment (Goto and Hayashi, 1997; Kubota et al., 2000). The wing and leg discs are then separated dorsoventrally by what appears to be the dorsal

* Corresponding author. Riken Center for Developmental Biology, 2-2-3 Minatojima-minamimachi, Chuo-ku Kobe 650-0047, Japan. Fax: +81 78 306 3183.
E-mail address: shayashi@cdb.riken.jp (S. Hayashi).

0012-1606/$ - see front matter © 2006 Elsevier Inc. All rights reserved.
doi:10.1016/j.ydbio.2006.12.022

migration of the wing disc (Cohen et al., 1993). Both primordia then invaginate to form the imaginal discs. As we describe here, following invagination, the wing disc becomes elongated and attaches to the tracheal system. The *Drosophila* tracheal system is also derived from ectodermal invaginations, which form tubules that are connected in a complex network to supply oxygen to the internal tissues (Samakovlis et al., 1996). Although it has been reported that the attachment of the wing imaginal disc to the tracheal branches starts during embryogenesis (Bate and Martinez-Arias, 1991), when and how the tracheal branches become associated with the wing discs is unknown.

The wing disc gives rise to the dorsal part of the adult mesothorax, which includes the wing and the notum, and encases the musculature that powers flight. The activity of this musculature is supported by the air sac, a highly developed tracheal system that ramifies within the notum during the late third larval instar (Guha and Kornberg, 2005; Sato and Kornberg, 2002). Thus, the association of these tissues with the wing disc during embryogenesis is important for the development of the adult flight system.

We demonstrate that elongating wing disc cells associate tightly with the tracheal cells by forming structures with closely apposed basal cell membranes. Live imaging reveals that this association is highly dynamic and that the wing disc cells behave like migrating cells in culture. We show that the α1,2 laminin Wb, which is produced in the wing disc, and integrins are essential for the proper association between the wing disc and the trachea, and for migratory cell behaviors. The identification of the genes that control the shape and position of the wing disc provides insight into the tissue interactions between the wing disc and tracheal branches.

Materials and methods

Fly strains

The following fly strains were used: *Dll-Gal4* (Calleja et al., 1996), *esg-Gal4* (Hayashi et al., 2002), *btl-Gal4* (Shiga et al., 1996), *UAS-tau-gfp* (Micklem et al., 1997), *UAS-gfp-moesin*, *UAS-Drac1*^{V12} (Luo et al., 1994), *sGMCA* (Kiehart et al., 2000), *1-eve-1* (*trh-lacZ*) (Kassis et al., 1992), *btl-gfp-moesin* (Kato et al., 2004), *btl*$^{\Delta 10}$ (Ohshiro and Saigo, 1997), *bnl*^{1} (Sutherland et al., 1996), *trh*^{1} (Llimargas and Casanova, 1999), *mys*^{XG43}(Bunch et al., 1992), *LanA*$^{9\text{-}32}$ (Henchcliffe et al., 1993), and *if*^{B4} (Brown, 1994). *UAS-gfp*^{S65T}, *UAS-gfp-NLS,* and *wb*^{09437} were obtained from the Bloomington Stock Center.

Time-lapse observations

Dechorionated embryos were mounted on a glass-bottomed dish (Iwaki, Chiba, Japan; 3910-035) with rubber cement, covered with water, and observed with a confocal laser-scanning microscope (Olympus Corporation, FV-300 multi-point) equipped with a 60× oil immersion lens (NA1.42), in a room maintained at 22 °C. Typically, 10 2-μm-thick z-stacks were taken every 1–2 min over a period of 4 h. In some cases, the genotype of the recorded embryos was determined retrospectively by scoring the terminal phenotype.

Fluorescence microscopy

The following primary antibodies were used: anti-Esg (Fuse et al., 1994), anti-Dlg (Developmental Studies Hybridoma Bank, University of Iowa) anti-Wb (Martin et al., 1999), mouse anti-βPS (6G11; Developmental Studies Hybridoma Bank), rat anti-βPS (anti-BG1; a monoclonal antibody that detects the β subunit when it is in a complex with αPS2; (Hirano et al., 1991), rabbit anti-green fluorescent protein (GFP; MBL), and anti-β-galactosidase (Cappell Laboratories, Pennsylvania). A mouse polyclonal antibody directed against the globular domains of LanA was kindly provided by Dr. Yasumitsu Takagi, Fukuoka Dental College (unpublished). The signal was sometimes amplified with a TSA-Indirect kit (NEN Life Science Products, Boston Massachusetts). Images were recorded using a confocal microscope (Olympus FV-500).

Whole-mount in situ hybridization

In situ hybridization of whole-mounted embryos was performed essentially as described previously (Tautz and Pfeifle, 1989), using a digoxigenin-labeled RNA probe for *wb* cDNA (nucleotide 660–1401).

Transmission electron microscopy

Control (*y w*), *mys*, and *wb* embryos were fixed by high-pressure freezing and freeze substitution, as described previously (McDonald, 1994). *mys* mutant embryos were identified by the phenotype of dorsal closure. *wb* mutant embryos were identified from a cross between stocks carrying recombinant chromosomes of either *wb UAS-gfp-moesin* or *wb btl-Gal4*. GFP-positive embryos were picked up for TEM analyses. Standard protocols were used for sample preparation, dissection, and observation. The association of the wing disc with the trachea was examined in at least 30 sections (100 nm) that included the wing disc.

Results

Dorsal displacement of the wing disc cells in the ectoderm

The early stage of wing disc development in living embryos was observed by tracing the movement of wing primordial cells labeled with GFP expressed under the *Dll* enhancer (*Dll>GFP*) (Bate and Martinez-Arias, 1991; Kubota et al., 2000). In the period spanning stages 12 to 14, GFP-expressing cell clusters in each thoracic segment extended in the dorsoventral direction (Figs. 1A–C). By stage 15, the wing disc cells were well separated from the leg primordia (Fig. 1D). This and all other descriptions of the wing disc also apply to the haltere disc. Hereafter, we will collectively call the two dorsal thoracic discs the ‘wing disc’. We also observed a dorsal cluster of GFP-positive cells in the prothorax, which may give rise to the dorsal prothoracic disc.

To determine whether the dorsal shift of the wing disc cells is an active cell migration, we followed the positions of the wing disc cells relative to those of the surrounding ectodermal cells (Figs. 1E, F, supplemental movie 1). During a 1 h period within stage 12, the *Dll>GFP*-expressing cell cluster extended ~1.5-fold in length along the dorsoventral axis. Cell tracing demonstrated that the relative positions of the *Dll>GFP*-expressing cells (green) and neighboring ectodermal cells (magenta) did not change, although the cells elongated along the dorsoventral axis (Figs. 1E, F). Analyses of stage 13–16 embryos using the wing disc marker *escargot (esg)* led us to the same conclusion (Figs. 1G–I; compare the positions of the blue-labeled wing disc cells with the ectodermal cell indicated by the white asterisk). At stage 16, when the invagination of the wing and leg discs was apparent, the cells in the intermediate position (labeled green) remained in the ectoderm and separated the wing and leg discs (Fig. 1I), as previously proposed (Goto and

Hayashi, 1997). We concluded that little cell rearrangement took place in the region surrounding the wing disc, and therefore the apparent dorsal movement of the wing disc is probably a passive process attributable to cell stretching in the ectoderm. Instead, the leg disc clearly migrates ventrally relative to nearby ectodermal cells (Figs. 1G–I).

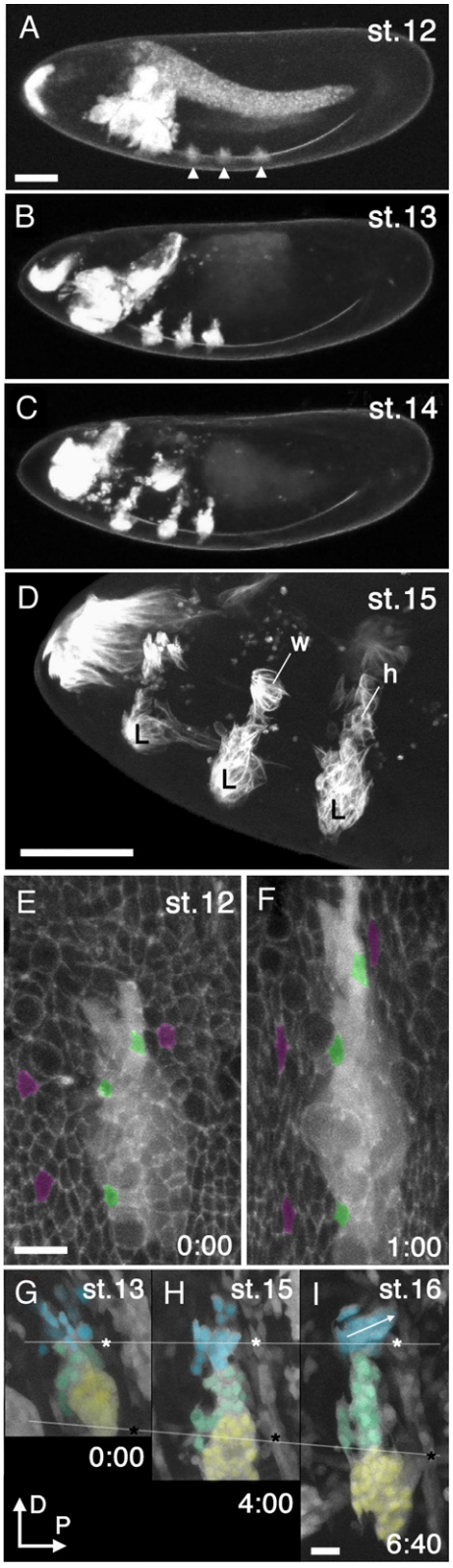

Cytoskeletal reorganization in the wing disc

Although the separation of the wing disc from the leg disc was not an active process, the wing disc cells apparently moved posteriorly during invagination (Fig. 1I, arrow). Therefore, we next studied the process of wing disc invagination by visualizing the movement of the nucleus (nuclear localization signal [NLS]-GFP), microtubules (tau-GFP), and F-actin (GFP-moesin; Fig. 2; supplemental movies 2–4). At early stage 14, microtubules in the cells of the prospective wing disc region, which had been randomly oriented in the plane of the ectoderm (Fig. 2B, 0:00), began to polarize along the anterior–posterior axis (Fig. 2B, 0:30). At late stage 14, a cluster of nuclei in the prospective wing disc region started to move posteriorly (Fig. 2A, 0:30, arrow). We also observed a clustering of nuclei in the leg region (Fig. 2A, 2:00, yellow), which showed some degree of microtubule alignment (Fig. 2B, 2:00, yellow). However, we did not detect any microtubule polarization or clustering of nuclei in the intermediate region between the wing and leg discs (Figs. 2A and B, 2:00, green).

Basal filopodial activities in the wing disc

Examination of the invaginating wing discs in stages 14–15 revealed prominent accumulation of F-actin and the extension of filopodia at the basal cortex (Fig. 2C, 0:30–2:00, insets, supplemental movie 4). The accumulation of F-actin was strongest on the posterior side (Figs. 2D, D′). Time-lapse images of elongating wing discs indicated that the filopodial activity persisted until stage 16, albeit at a reduced level (Fig. 2E, arrowheads, Fig. 3A, supplemental movie 5). F-actin also accumulated at the apical constriction of the invaginating wing disc during stages 14–16, suggesting that the cells retained epithelial characters (Figs. 2C–E, asterisks).

Fig. 1. (A–C) A *Dll-Gal4/UAS-gfp* (*Dll>gfp*) embryo in three successive stages. Lateral view, anterior is left, dorsal is up. (A) Germ-band retraction has begun. The limb primordia are indicated (arrowheads). (B) Germ-band retraction is complete (time, 3 h 20 min since A). (C) Beginning of head involution (time, 7 h 20 min since A). (D) Thoracic region of *Dll>tau-gfp* embryo at stage 15. The limb primordium has elongated in the dorsoventral direction and segregated the wing (w), haltere (h), and leg (L) discs. (E, F) Dorsoventral extension of the limb primordium during germ-band retraction. The second thoracic segment was simultaneously labeled with *Dll>GFP* and *sqh-gfp-moe (sGMCA).* (E) Germ-band retraction has begun. The stage here is approximately the same as that shown in panel A. Cells in the lateral epidermis have a polygonal shape (magenta), as do those in the limb primordium (green). (F) Germ-band retraction is almost complete after 1 h. Marked cells have elongated in a dorsoventral direction, as has the limb primordium. The relative positions of the marked limb primordial cells and epidermal cells did not change. (G–I) The wing primordium does not migrate dorsally during dorsal closure. Time-lapse images of a *Dll>gfp, esg>gfp* embryo from stage 13 to stage 16. The fate of each GFP-positive cell was identified by following it to the end of embryogenesis. The cells were pseudo-colored blue (wing), yellow (leg), or green (larval epidermis). By comparison with the position of an epidermal cell (white asterisk), it was concluded that the wing disc cells (blue) did not change their positions relative to those of the flanking epidermal cells. However, the leg disc cells shifted ventrally relative to another epidermal cell (black asterisk). (I) Note the anteroposterior elongation of the wing disc cells (arrow). Time is shown in hours:minutes from the time the first image was recorded. Bar: 50 mm (A–D), 10 mm (E–G).

Wing discs elongate by migration over tracheal branches

The presence of basal filopodia in the wing disc cells is unusual for typical epithelia and resembles the behavior of migrating cells. Because the wing discs come to associate with the tracheal system during stages 15–16 (Bate and Martinez-Arias, 1991), the filopodia of the wing disc cells may reflect the process of association with the trachea and/or target searching prior to the association. Indeed, at the onset of invagination at stage 13, filopodia from the wing disc cells made contact with the lateral trunk anterior (LTa, *) tracheal branch (Figs. 4B-i,iii, D, E), suggesting that this may be the first step in target tissue searching. We also observed that tracheal cells decorated with numerous filopodia spread over the basal surface of the wing disc at stage 14 (Fig. 4G). During elongation, the basal part of the wing disc cell extended its site of contact to the lateral trunk posterior (LTp, **), then to the spiracular branch (SP, ***) and the transverse connective (TC, ****), which are located more posteriorly (Figs. 4C, D–F), and remained in this position by metamorphosis (data not shown). We also noted that the basal filopodia of the wing disc cells at stage 16 were almost always in close contact with the trachea (Fig. 4C-iii, arrowheads). These observations suggest that the filopodia extending from the wing disc may play a role in actively searching for the trachea and/or in migration over it.

We quantified the relative positions of the wing disc and tracheal branches using arbitrary defined M index ($M=(B+2xC)/(A+B+C)$, A, B, and C indicate wing disc area on projection images, Fig. 4H). The movement of the wing disc cells proceeded slowly during stages 14–15, and became rapid in stage 16 (Fig. 4I). The small variation in the M index suggests that the elongation of the wing disc is a highly reproducible process.

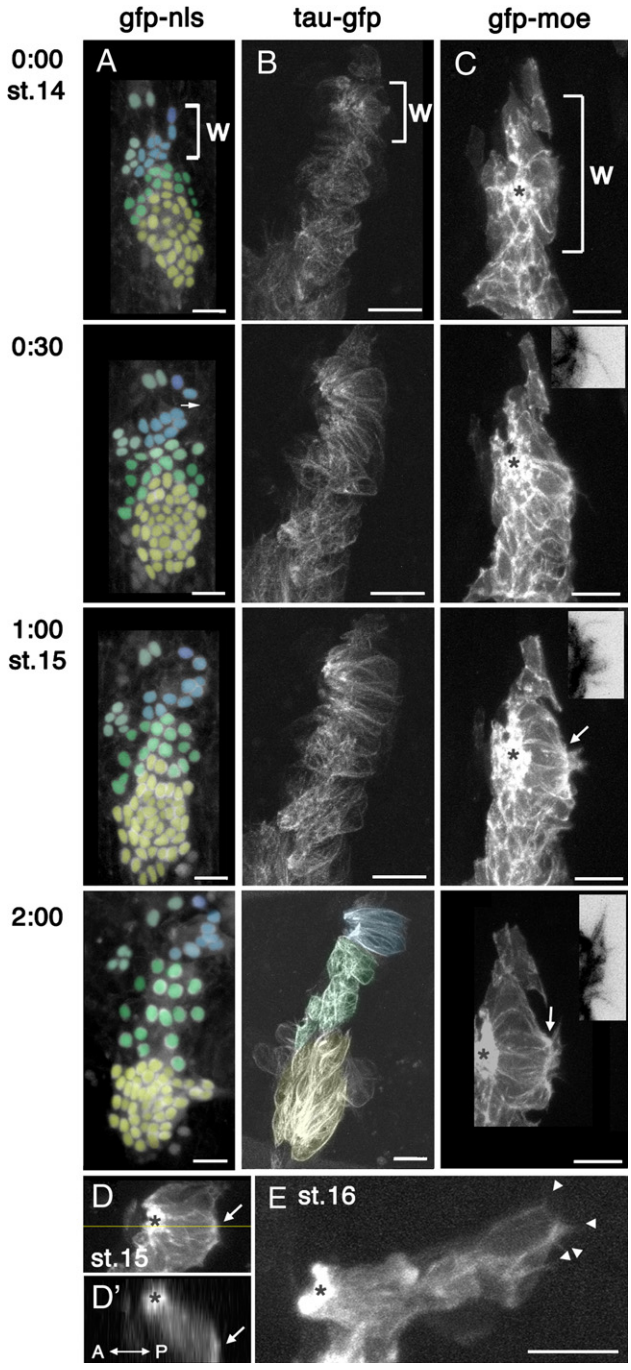

Fig. 2. Time-lapse analyses of cytoskeletal changes during wing disc formation. Between 13 and 15 z-sections were taken at each time point and were projected to produce xyz-t stacks. The position of the wing primordium is indicated (w). (A) Limb primordial cells labeled with GFP-NLS are pseudo-colored according to their final fate. Presumptive wing (blue), leg (yellow), and larval epidermis (green) are shown. The time elapsed in hours:minutes is indicated at the left of each image. The wing disc cells start to move posteriorly relative to the other cells (A, 0:30). (B) *Dll>tau-GFP.* In the 2:00 frame, the cells are pseudo-colored according to their fates. In the wing disc (blue), the microtubules became aligned and oriented in an anterior–posterior direction, whereas in the presumptive larval epidermal cells (green), the microtubules remained randomly oriented. (C–E) The pattern of F-actin visualized with *Dll>GFP-moesin.* (D′). A transverse optical section of panel D shows that F-actin accumulated on the posterior side of the wing disc in stage 15. Notice that the wing disc cells show a strong accumulation of F-actin on their posterior sides (C, D, arrows). Asterisks indicate the positions of the apical constriction that is connected to the epidermis. Insets in panel C show enlarged views. Bar: 10 μm.

Tracheae are required for the elongation of the wing disc

To examine whether the trachea contributes to the formation or positioning of the wing disc, we examined *trachealess* mutant embryos (trh^1) (Isaac and Andrew, 1996; Wilk et al., 1996). In the total absence of tracheae, the wing disc cells normally formed apical constrictions and elongated apicobasally, as observed in wild-type embryos (Figs. 5B, B′), suggesting that wing disc invagination occurs independently of its association with the trachea. However, the elongation of the wing disc was abnormal. The wing discs were often bent, extended basal filopodia in abnormal directions, and failed to elongate to the level of the control discs (Figs. 3D, E). We also examined the position of the wing disc after it was fully extended in late stage 16 (Figs. 5C, D). In control embryos, the wing disc remained in a fixed position despite the peristaltic muscular activity, as revealed by the little variation in the angle of the wing disc relative to the epidermis (Fig. 5C). In trh^1 embryos, the position of the wing disc was highly unstable (Fig. 5D), suggesting that its association with the trachea is essential

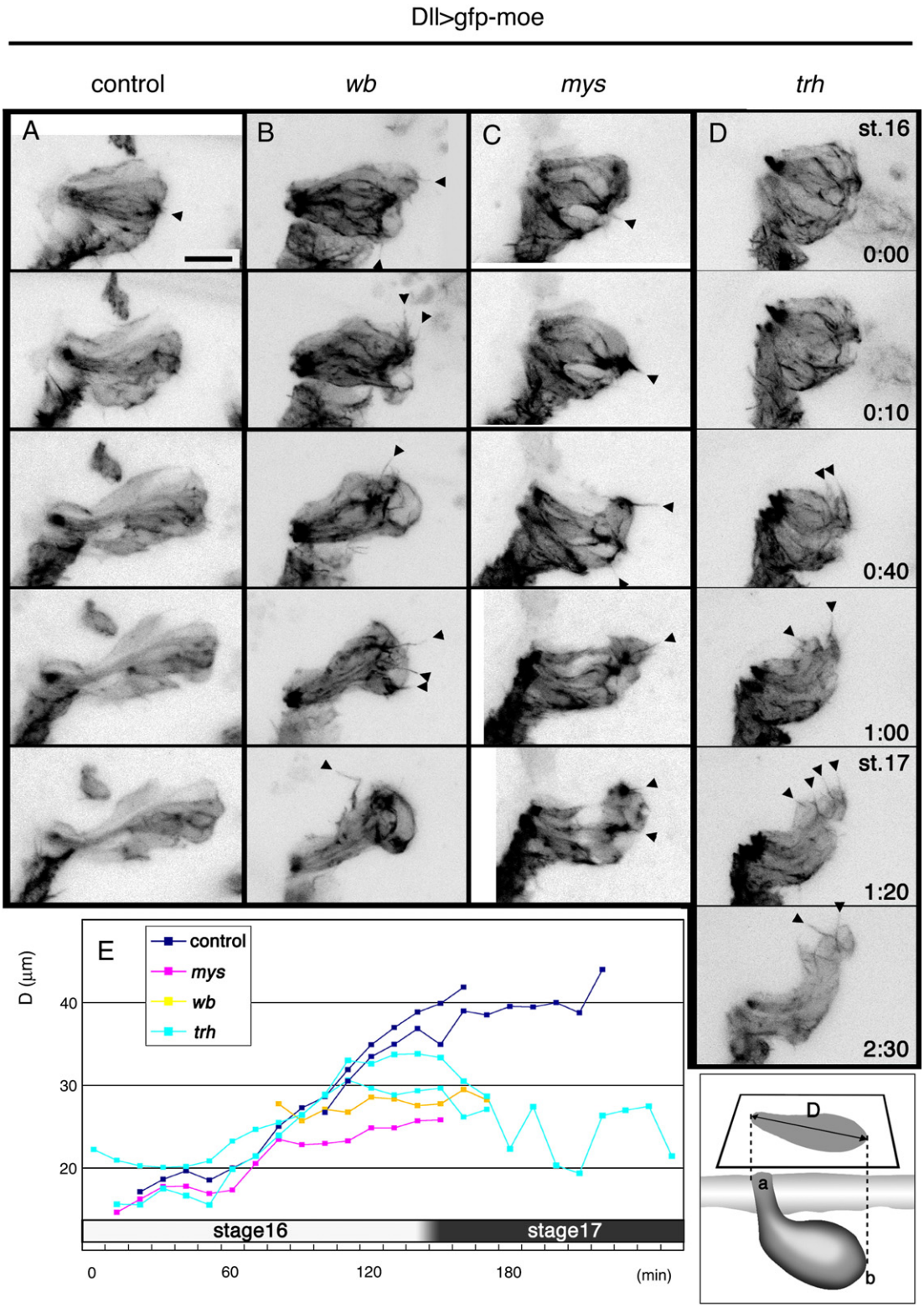

Fig. 3. Time-lapse images of the wing discs labeled with the F-actin marker GFP-moesin during the rapid elongation phase in stage 16. Control (A), *wb* (B), *mys* (C), and *trh* (D). (A) Accumulations of F-actin and filopodia (arrowheads) were observed in limited basal positions (A; 0:00), but they were reduced in later stages. (B–D) Filopodia persisted and were sometimes misoriented in the *wb*, *mys*, and *trh* mutants (arrowheads). In the *trh* embryo, the wing disc was bent dorsally. (E) Measurement of wing disc elongation. As shown in the schematic (right), the distance (D) between the apical constrictions (a) and the basal end (b) of the wing disc was measured in the projection images of embryos (lateral view) at 10 min intervals. The length of the wing disc in the control embryos increased steadily from ~20 μm to ~40 μm in stage 16. In *mys*, *wb*, and *trh* mutant embryos, the wing disc elongation stalled prematurely. Bar: 10 μm.

to stabilize the position of the wing disc so that it can withstand the vigorous muscular activities of peristalsis.

We next examined whether the wing disc–trachea interaction requires fibroblast growth factor (FGF) signaling, which is known to be important for the migration of tracheal branches and their association with the larval wing disc (Ghabrial et al., 2003; Guha and Kornberg, 2005; Sato and Kornberg, 2002). Mutations in the FGF receptor (*btl*; Klambt et al., 1992; Fig. 5E) caused the arrest of tracheal branching immediately after invagination. The wing discs invaginated in the *btl* mutants, and they associated with the tracheae in most cases. A similar result was obtained with mutants of the FGF ligand (*bnl*; Sutherland et al., 1996; data not shown), suggesting that FGF signaling is not essential for the wing disc–trachea association. We also used an activated form of Rac to disrupt the tracheal epithelium (Chihara et al., 2003), and found that the wing disc was still attached to mesenchyme-like tracheal cells, the positions of which had moved anteriorly (Fig. 5F). These results suggest that the position of the wing disc depends on the proper patterning of the tracheal branches.

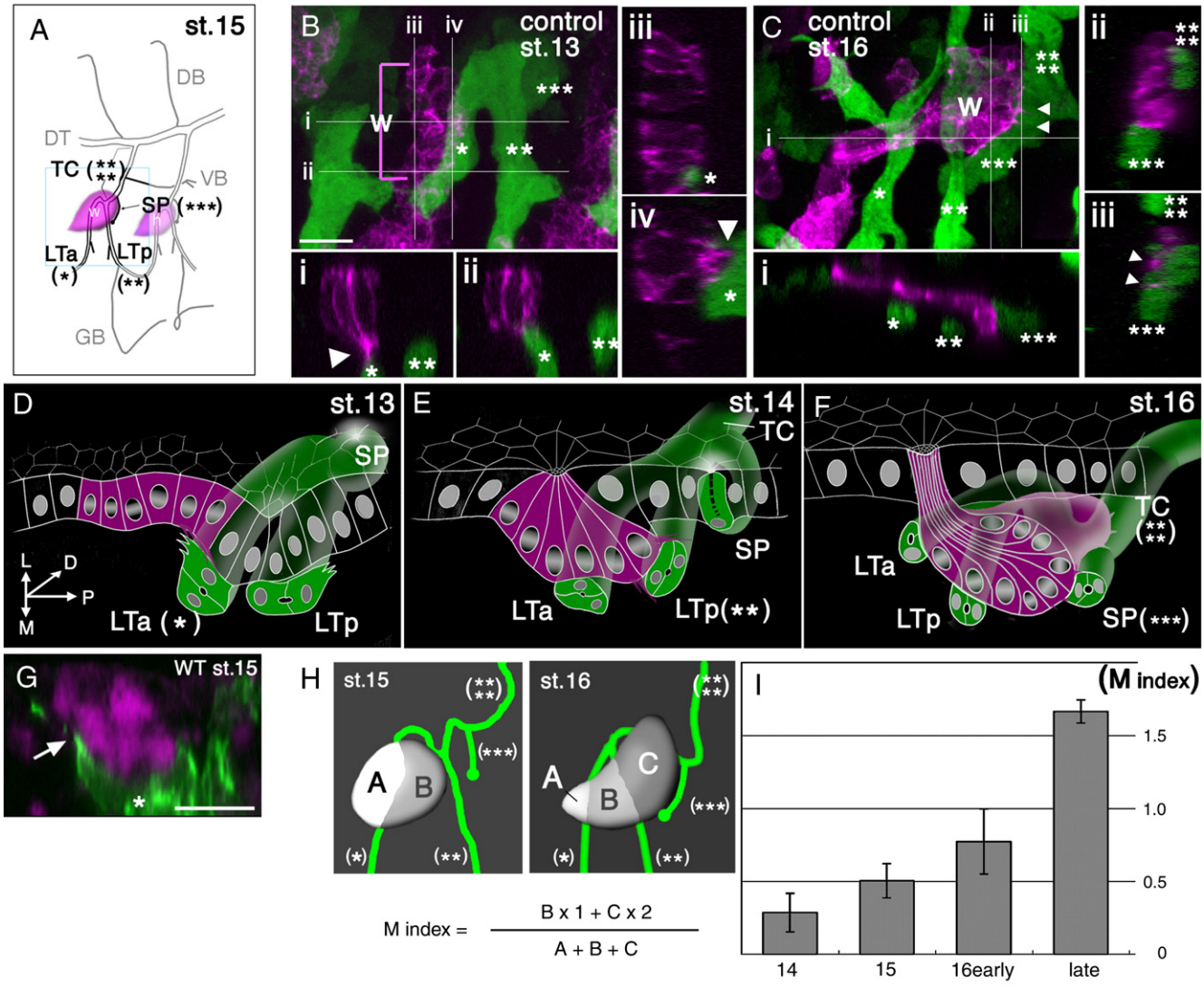

Fig. 4. Association of the wing disc with the trachea. (A) Diagram of the tracheal branches and wing disc in stage 15 (lateral view, anterior left). DB, dorsal branch; DT, dorsal trunk; GB, ganglionic branch; VB, visceral branch; LTa (*), lateral trunk anterior; LTp (**), lateral trunk posterior; SB (***), spiracular branch; TC (****), transverse connective. Notice that the wing disc (w; T2) attaches to the T3 tracheal metamere, and the haltere disc (h; T3) to the A1 metamere. (B–C) Association of the wing disc with underlying tracheal branches in stage 13 (B) and stage 16 (C). The wing disc cells are labeled with *Dll>GFP-moe* (magenta). Tracheal cells are labeled with *trh-lacZ* (green). Anterior is left. The white lines (i, ii, iii, and iv) in panels B and C indicate the plane of the z-sections (Bi–iv, Ci–iii). Panels B and C are at the same magnification. Bar: 10 μm. (D–F) Diagrams of the relationship between the tracheal branches and wing discs (anterior left). At stage 13, invaginating wing discs first attach to LTa (*)(D). At stage 15, the wing disc cells elongate apicobasally, extend anterior–posteriorly, and associate with LTp (**). (E). At stage 16, the elongated wing disc cells associate with SP (***) and TC (****) (F). (G) A sagittal optical section of an embryo carrying *btl>gfp-moe* (green). The wing disc cells were stained with anti-Esg antibody (magenta). Tracheal cells extended filopodia and spread over the basal surface of the wing disc (arrows). Bar: 10 μm. (H) Diagram showing the definition of the migration (*M*) index. From projected confocal images, three sectors of the wing disc (A–C), defined by their positions relative to LTa (*) and LTp (**), were identified and their areas were measured. The *M* index was calculated for each image using the equation shown below the figure. Asterisks indicate tracheal branches according to panel A. (I) Measurement of the *M* index in control embryos demonstrated that the value increased gradually during stages 14 and 15, and then increased rapidly during stage 16. Bars indicate standard deviations (>15 embryos counted).

Specific expression of a laminin α subunit in the wing disc

Because the wing disc and trachea contact each other at the basal cell surface, which is covered with the ECM, we reasoned that a change in ECM content might play a regulatory role in the wing disc–trachea interaction. *Drosophila* has two laminin isoforms, which are distinguished by two types of α subunits, α3,5 (*LanA*) and α1,2 (*wing blister; wb)*, which each form a trimer with the common β and γ subunits (Fessler et al., 1987; Kusche-Gullberg et al., 1992; Martin et al., 1999). LanA (Henchcliffe et al., 1993) started to accumulate in and around the trachea at stage 14 (Fig. 6A). The cytoplasmic LanA signal suggests that it is produced by the tracheal cells. In contrast, mRNA for *wing blister (wb)*, which encodes the other laminin α subunit (Martin et al., 1999), was detected strongly in the wing disc (Fig. 6B). Beginning at stage 14, Wb protein was detectable in the cytoplasm of the wing disc cells and at the interface of their contact with the tracheal cells (Figs. 6C, D). Wb was not detected in the tracheal cells or in the surrounding larval epidermis (Fig. 6C). Thus, distinct laminin α subunits are associated with the wing disc and the trachea when they contact each other. Other ECM components, such as collagen IV and tiggrin, were not detected in association with the wing discs or tracheae (data not shown).

We also examined the expression of integrin using two monoclonal antibodies directed against βPS (BG-1 and 6G11). Both antibodies detected signals near the site of contact between the wing disc and the trachea (Fig. 6E, and data not shown). Double labeling revealed that the βPS signals colocalized with a subset of Wb signals at the margin of wing disc cells in association of tracheal branches (Fig. 6F, arrowhead). The rest of Wb signals were found inside of the wing disc (Fig. 6F). We further examined the mutual dependence of the localization of Wb and βPS (Figs. 6G–H). At the wing disc–trachea interface, the Wb accumulation was reduced in mutants of the βPS subunit (*myospheroid* [*mys*]) (Fig. 6G), and βPS accumulation was reduced in *wb* mutants (Fig. 6H), indicating that colocalization of Wb and βPS at the wing disc–trachea interface is mutually dependent.

Defective wing disc elongation in embryos deficient in laminin or integrin

To investigate the roles of laminin and integrin in the wing disc–trachea interaction, we examined the zygotic mutant phenotypes for the laminins (*wb* and *LanA*) and the two integrin subunits, βPS (*mys*) and αPS2 (*if*) (Figs. 6I–N). These mutants allowed the wing disc to invaginate with the normal number of

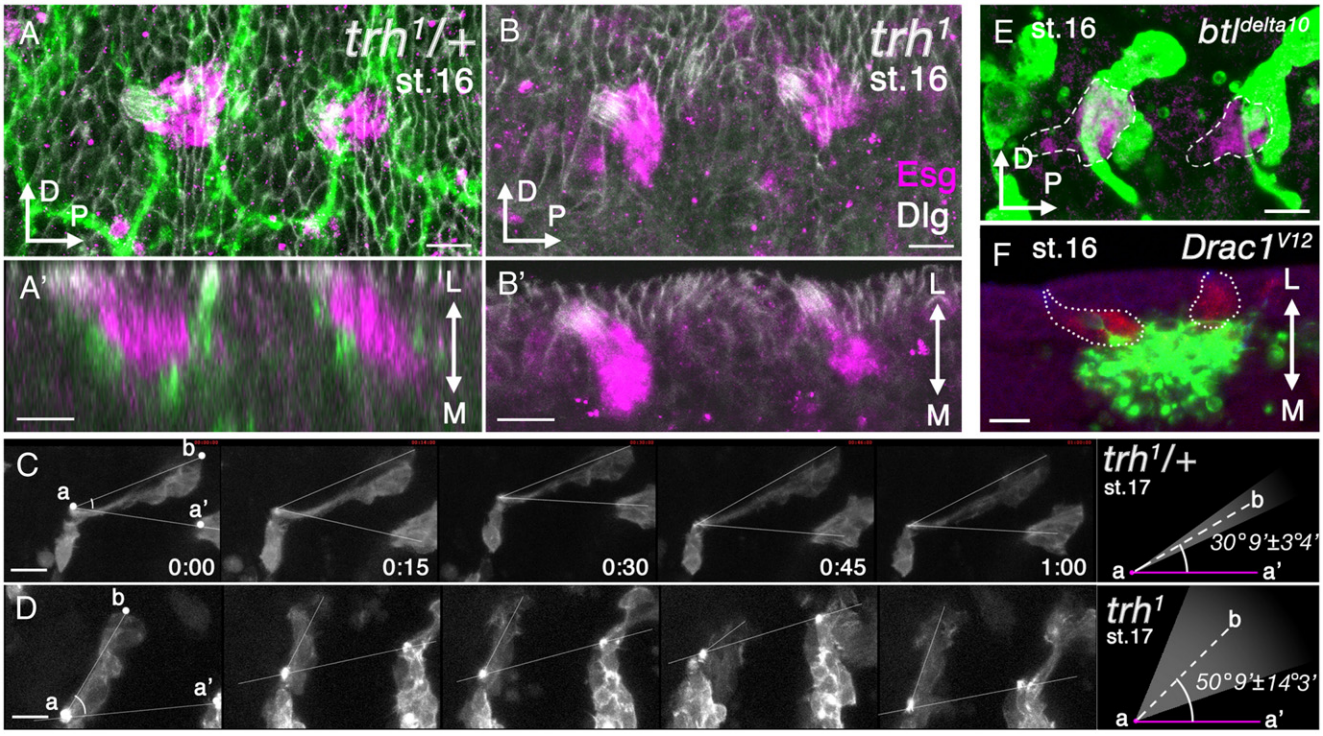

Fig. 5. The position of the wing disc depends on the trachea. (A, B) The wing disc invaginated normally in both control trh^1/+ and trh^1 embryos. Embryos were labeled with *btl-gfp-moe* (green), Esg (magenta), and Dlg (white). Panels A′ and B′ are x–z sections. D, dorsal; P, posterior; L, lateral; M, medial. (C, D) Mislocalization of the wing disc in the absence of the trachea. Series of still images from projected confocal stacks of living embryos at stage 17 showing the movement of wing discs in the control (C; trh^1/+) and the *trh* mutant (D; trh^1). Anterior left, dorsal up. Line a–a′ connects the apical constrictions of the wing and haltere discs. Line a–b connects the apical constriction to the basal end of the wing disc. The angle b–a–a′ corresponds to the dorsal tilt of posteriorly oriented wing discs and was measured every 15 min over 1 h of recording. It remained constant in the control embryos despite active muscular contractions, but varied considerably in the trh^1 embryos. (E) A $btl^{delta10}$ embryo. In the absence of FGF signaling, the wing disc extended and associated with stalled tracheal cells. (F) Disruption of the tracheal epithelium by $rac1^{V12}$. The haltere disc migrated toward the mislocated mesenchymal tracheal cells. Bar: 10 μm.

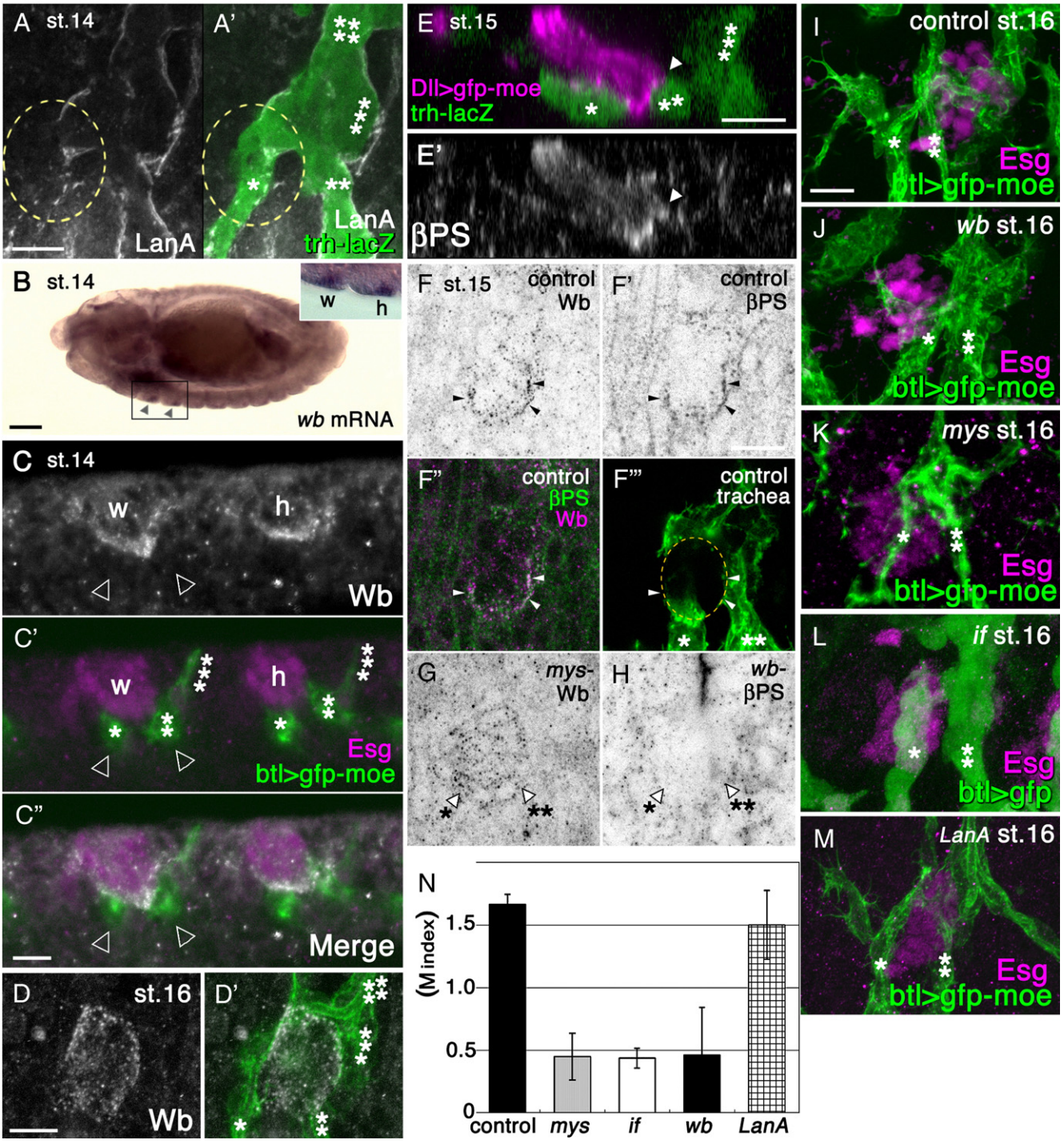

Fig. 6. Laminin and integrin are required for the elongation of the wing disc. (A) LanA expression was detected in the trachea, but not in the position of the wing disc (dotted line). Asterisks indicate tracheal branches according to Fig. 4A. (B) *wb* mRNA expression in wing (w) and haltere (h) discs in a stage 14 embryo. Dorsolateral view, anterior is left. (C, D) Expression of Wb protein in wild-type embryos (gray scale images in panels C, D). Wing (w) and haltere (h) cells were labeled with an anti-Esg antibody (magenta in panels C′ and C″). Wb accumulated in the cytoplasm of the wing disc cells and at the attachment site between the wing and trachea. (E, E′) βPS detected with anti-βPS antibody (BG-1) accumulated at the attachment site between the wing and trachea (E′). (F, F′, F″, F‴) Localization of βPS and Wb. A wing disc labeled with Wb (F) and βPS (F′) is shown. Overlap of those signals at the position facing the trachea (arrowhead) appears white in the two color panel (F″; WB, magenta; βPS, green). The location of the trachea (green) and the position of the wing disc (outlined by the yellow dotted line) were shown in panel F‴. (G, H) Localizations of βPS and Wb are mutually dependent. At the interface of the wing disc and trachea that was identified by the location of the tracheal branches (arrowhead, not shown for clarity), Wb accumulation was reduced in *mys* mutants (G) and βPS was reduced in *wb* mutants (H). (I–M) Elongation of the wing disc was impaired in *wb*, *mys*, and *if* mutants, but not in *LanA* mutants. (N) Quantification of the phenotypes shown in panels I–M. Tracheal cells were labeled with *trh-lacZ* (A, E), *btl>gfp-moe* (C′, C″, D′, I–K, M), or *btl>gfp* (L), and are shown in green. Bar: 10 μm (A, C–M), 50 μm (B).

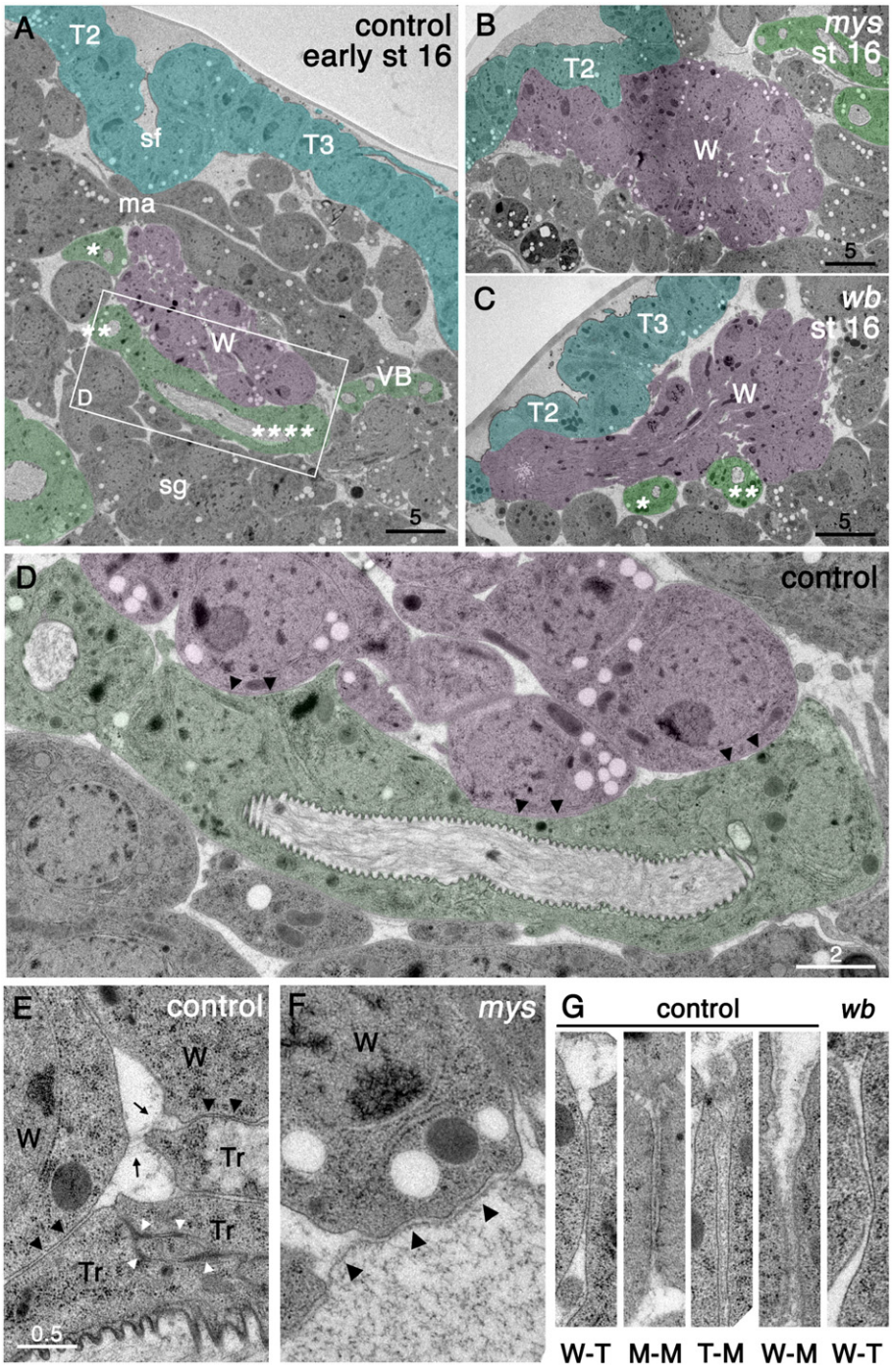

Fig. 7. TEM analyses of the wing disc–trachea association. (A) A sagittal section of a control embryo at early stage 16 provides a general morphological overview of the wing disc and surrounding tissues. Anterior is left, lateral is up. Green, tracheal cells; magenta, wing disc cells; blue, epidermis. The wing disc cells are separated from the epidermis by the presence of the muscle and fat body, except at the apical cell junction connected to the epidermis, which is located outside this section. Asterisks indicate tracheal branches according to Fig. 4A. VB, visceral branch; ma, muscle attachment site; sf, segmental fold between T2 and T3; sg, salivary gland cells. Box indicates the region magnified in panel D. (B, C) In the *mys* and *wb* mutants, wing disc cells rarely associated with the tracheal cells. Ectopic contact of the wing disc cells with the basal surface of the epidermis was observed in both cases. (D) Enlarged view of the boxed region in panel A, showing the tight association between the wing disc and tracheal cells (arrowheads). (E) The wing disc and trachea formed an interface with tightly apposed plasma membranes (arrowhead). String-like structures often bridged the wing disc and tracheal cells (arrows). Tracheal cells attached to each other at their lateral surfaces with septate junctions (white arrowheads). (F) High-magnification image of the *mys* mutant. The ECM is detached from the basal surfaces of the wing disc cells (arrowheads). (G) Comparison of the extracellular spacing between various cell types. Between the wing and trachea (W–T), a constant extracellular space of 26 nm was observed. The interfaces between longitudinal myotubes (M–M), between the trachea and mesodermal cells (T–M), and between the wing and mesodermal cells (W–M) were wider (up to 100 nm wide) and variable, and the extracellular space was filled with electron-dense material. In the *wb* mutant, the tight cell contact with the 26 nm spacing was not seen between the wing and tracheal cells (W–T). Bar: 5 μm (A–C), 2 μm (D), 0.5 μm (E–G).

cells, and the tracheal branches LTa, LTp, SP, and TC to be present in their normal locations. However, elongation of the wing disc in *wb*, *mys*, and *if* mutant embryos stalled in mid stage 16 (Figs. 6J–L, and N). Conversely, we detected no significant change in wing disc elongation in the *LanA* mutants (Figs. 6M and N).

We next examined time-lapse images of the wing discs of the *wb* and *mys* mutants (supplemental movies 6, 7). In both mutants, wing disc elongation and the movement of the basal filopodia appeared normal until stage 15. However, at stage 16, when the basal filopodial activity was downregulated in the control embryos (Figs. 3A, 1:00, supplemental movie 5), the filopodial activity remained constant in the *wb* and *mys* mutants (Figs. 3B–C, arrowhead). Those phenotypes resembled the phenotype of the trh^1 mutant (Fig. 3D, supplemental movie 8) and suggest that Wb and βPS are required for the down-regulation of the basal filopodia. Quantification confirmed that the wing disc elongation in the *wb* and *mys* embryos stalled in mid stage 16, as observed in the trh^1 embryos (Fig. 3E).

Ultrastructural analyses of cell adhesion between the wing disc and trachea

To understand how deficiencies in Wb or integrin activities affect the cell adhesive properties of the wing disc–trachea interaction, we used electron microscopy to analyze stage 16 embryos (Fig. 7). High-pressure freezing combined with freeze substitution allowed us to visualize the adhesion structures and the ECM. In control embryos at mid stage 16, when the filopodial movement had decreased and rapid wing disc elongation was still in progress, we observed close contact between the wing disc and the trachea (Fig. 7D, arrowheads). The apposing plasma membranes were separated by a parallel gap of 26.06±0.03 nm widths, which was often observed in consecutive 100-nm-thick ultrathin sections, suggesting that the wing disc and tracheal cells make contact over a large surface area (Fig. 7G). The interface between the longitudinal myotubes, tracheae, and myotubes, and between the wing discs and myotubes were wider and more variable in length, suggesting that the trachea–wing disc interface is a specific structure (Fig. 7G). The ECM was observed as an electron-dense material covering the surfaces of the wing disc and the trachea and their vicinities (Figs. 7D, G). It was sometimes observed as string-like structures (Fig. 7E, arrows).

In the *mys* and *wb* mutant embryos, the wing disc and trachea were usually separated by a large space (Figs. 7B, C). In rare cases when the two tissues made contact, the spacing between the two cell types was irregular and the area of close contact was limited to small spots (Fig. 7G). Thin layers of electron-dense structures were also observed in the extracellular space near the wing disc (Fig. 7F). These were probably ECM detached from the basal surface of the wing disc. These phenotypes suggest that the formation of the large area of cell–cell contact with the 26 nm gaps depends on Wb and integrins. From the results of both TEM and time-lapse imaging, we suggest that the large attachment area of cell–cell contact might provide a basis for the traction force of the elongating wing disc cells.

Discussion

The integrin–ECM interaction is a key determinant of tissue interactions during organogenesis (Bradley et al., 2003). A multitude of integrin subunits and ECM components are differentially expressed, raising the possibility that the differential utilization of specific integrin–ECM combinations contributes to the specificity of tissue interactions. Boube et al. showed that the *Drosophila* embryonic midgut and visceral tracheal branches express the αPS2 and αPS1 integrin subunits, respectively, and that these subunits are required for the midgut–trachea interaction, suggesting that the differential expression of integrin subunits may contribute to specific tissue interactions (Boube et al., 2001). Here, we studied the roles of ECM components during the interaction of the wing disc and trachea, and demonstrated that one of the laminin subunits, Wb, expressed by the wing disc, plays a key role in cell adhesion and cell migration.

Role of the laminin–integrin interaction in directed tissue migration

Mammalian tissues produce at least 15 distinct laminin isoforms derived from combinations of five α, four β, and three γ subunits (Miner et al., 2004). The potential redundancy of these isoforms has so far complicated the functional analysis of the laminin isoforms in development. However, the smaller genome of *Drosophila* greatly simplifies the analysis of the laminin functions. LanA is widely distributed in the basement membrane of the epidermis, somatic and visceral muscles, and nervous system (Fessler et al., 1987; Kusche-Gullberg et al., 1992), whereas the expression of Wb is restricted more to the digestive system and muscle attachment sites (Martin et al., 1999).

We have shown here that Wb and LanA are expressed in a reciprocal manner in the wing disc and trachea during the critical stage of their association. Whereas Wb, αPS2, and βPS are required for wing disc elongation, LanA is not essential. Wb, but not LanA, contains the RGD integrin recognition motif (Graner et al., 1998). Since BG-1 binds to βPS complexed with αPS2 (Hirano et al., 1991), and αPS2 mutation *if* showed phenotype similar to that of βPS, αPS2βPS is an essential integrin heterodimer acting at the interface of the wing disc and the trachea. We have shown that βPS colocalized with Wb at the interface of the wing disc and trachea. Because this accumulation of Wb was reduced in the absence of βPS, Wb localization at the basolateral surface of the wing disc cells may involve an integrin-dependent capture mechanism. Consistent with this idea, we observed the detachment of the ECM from the basolateral surfaces of the wing discs of *mys* mutants. Taking these data together, we suggest that the recognition of the Wb laminin by the αPS2βPS integrin heterodimer facilitates the formation of the ECM, which mediates the interaction of the wing disc and the trachea, and modulates the migratory behavior of the wing disc cells.

Wing disc cells extended numerous filopodia in the early stage of migration, but the number and activity of the filopodia

was later reduced. This filopodial activity remained high in mutants lacking tracheae, integrins, or Wb laminin. We speculate that filopodial extension is an intrinsic property of wing disc cells, used to explore the target tissue, and that cell adhesion to the tracheal cells suppresses this filopodial activity via the signaling activity of integrins.

Electron microscopic analyses of the wing disc–trachea interface in stage 16 embryos revealed the presence of a cell–cell junction characterized by a 26 nm space, that was lost in the *wb* mutant embryos. One possible explanation is that integrins on the surfaces of two apposing cells sharing the same laminin molecule. The trimeric laminin molecule forms an asymmetric cross, consisting of three short (36 nm) arms and one long (77 nm) arm (Engel et al., 1981), with receptor-binding domains at each end. The ligand-binding head of the integrins is separated from the membrane by 12 nm (Carrell et al., 1985; Nermut et al., 1988). Since the configuration of integrins sharing of two of the short laminin arms would produce maximum spacing of 96 nm, an additional mechanism might be required to establish the junction with 26 nm spacing. We suggest that the Wb laminin produced in wing disc cells is captured at the cell surface by binding to the integrin receptor and is presented to tracheal cells. Wb laminin facilitates the cell–cell contact via integrin receptors and the signaling activity of integrins may repress the filopodial activity of the wing cells when the contact with the 26 nm gaps is broadly established. This large contact area provides the basis for the rapid cell migration that takes place in late stage 16.

Developmental significance of the wing–trachea attachment

The association between the wing disc and the tracheal system is an important step in the formation of a functional flight system (Sato and Kornberg, 2002; Whitten, 1980). This association takes place at the very beginning of wing disc development and is accompanied by the association of muscle precursor cells (Bate and Martinez-Arias, 1991; Bate et al., 1991; and Y.I., unpublished observation). This early association may reflect an ancient state of wing/notum primordia in hemimetabolous insects, in which adult structures develop in nymphs without imaginal disc intermediates.

The early association between the wing disc and tracheal system might provide an important advantage in holometabolous development. In the late larval and pupal stages, the wing disc grows into a flat structure that occupies the subepidermal space. It is connected to the epidermis by the peripodial membrane, which drives the evagination of the wing disc and the fusion of the pair of wing discs at the midline during the pupal stage (Fristrom and Fristrom, 1993; Pastor-Pareja et al., 2004). The elongation of the wing disc through its association with the trachea assures the precise placement of the wing disc in the body cavity. Thus, the trachea-mediated guidance of the wing primordium permits its growth and evagination during development. This mechanism may have contributed to the increase in wing size that occurred during the evolution of the holometabolous insects.

Acknowledgments

We thank Makiko F. Uwo and Shigenobu Yonemura (RIKEN, Center for Developmental Biology) for technical support for the TEM analyses, and Kagayaki Kato (RIKEN, Center for Developmental Biology) for help with image analysis; the Bloomington Stock Center, the Genetic Strain Research Center (National Institute of Genetics, Mishima, Japan), the Developmental Study Hybridoma Bank, Danny L. Brower (University of Arizona), Stefan Baumgartner (Lund University), and Yasumitsu Takagi (Fukuoka Dental College) for *Drosophila* strains and antibodies; and Nick Brown and Kiyoji Nishiwaki for helpful comments on the manuscript. This work was supported by a Grant-in-Aid for Scientific Research on Priority Areas “Systems Genomics” from the Ministry of Education, Culture Sports, Science and Technology, Japan, and a research grant from Japan Society for the Promotion of Science, Japan.

Appendix A. Supplementary data

Supplementary data associated with this article can be found, in the online version, at doi:10.1016/j.ydbio.2006.12.022.

References

Bate, M., Martinez-Arias, A., 1991. The embryonic origin of imaginal discs in *Drosophila*. Development 112, 755–761.

Bate, M., Rushton, E., Currie, D.A., 1991. Cells with persistent twist expression are the embryonic precursors of adult muscles in *Drosophila*. Development 113, 79–89.

Bökel, C., Brown, N.H., 2002. Integrins in development: moving on, responding to, and sticking to the extracellular matrix. Dev. Cell 3, 311–321.

Boube, M., Martin-Bermudo, M.D., Brown, N.H., Casanova, J., 2001. Specific tracheal migration is mediated by complementary expression of cell surface proteins. Genes Dev. 15, 1554–1562.

Bradley, P.L., Myat, M.M., Comeaux, C.A., Andrew, D.J., 2003. Posterior migration of the salivary gland requires an intact visceral mesoderm and integrin function. Dev. Biol. 257, 249–262.

Brown, N.H., 1994. Null mutations in the alpha PS2 and beta PS integrin subunit genes have distinct phenotypes. Development 120, 1221–1231.

Bunch, T.A., Salatino, R., Engelsgjerd, M.C., Mukai, L., West, R.F., Brower, D.L., 1992. Characterization of mutant alleles of myospheroid, the gene encoding the beta subunit of the *Drosophila* PS integrins. Genetics 132, 519–528.

Calleja, M., Moreno, E., Pelaz, S., Morata, G., 1996. Visualization of gene expression in living adult *Drosophila*. Science 274, 252–255.

Carrell, N.A., Fitzgerald, L.A., Steiner, B., Erickson, H.P., Phillips, D.R., 1985. Structure of human platelet membrane glycoproteins IIb and IIIa as determined by electron microscopy. J. Biol. Chem. 260, 1743–1749.

Chihara, T., Kato, K., Taniguchi, M., Ng, J., Hayashi, S., 2003. Rac promotes epithelial cell rearrangement during tracheal tubulogenesis in *Drosophila*. Development 130, 1419–1428.

Cohen, S.M., 1990. Specification of limb development in the *Drosophila* embryo by the positional cues from segmentation genes. Nature 343, 173–177.

Cohen, B., Simcox, A.A., Cohen, S.M., 1993. Allocation of the thoracic imaginal primordia in the *Drosophila* embryo. Development 117, 597–608.

Engel, J., Odermatt, E., Engel, A., Madri, J.A., Furthmayr, H., Rohde, H., Timpl, R., 1981. Shapes, domain organizations and flexibility of laminin and fibronectin, two multifunctional proteins of the extracellular matrix. J. Mol. Biol. 150, 97–120.

Fessler, L.I., Campbell, A.G., Duncan, K.G., Fessler, J.H., 1987. Drosophila laminin: characterization and localization. J. Cell Biol. 105, 2383–2391.

Fristrom, D., Fristrom, J.W., 1993. The metamorphic development of the adult epidermis. In: Bate, M., Martinez-Arias, A. (Eds.), The Development of *Drosophila melanogaster*, vol. 2. Cold Spring Harbor Laboratory Press, New York, pp. 843–898.

Fuse, N., Hirose, S., Hayashi, S., 1994. Diploidy of *Drosophila* imaginal cells is maintained by a transcriptional repressor encoded by *escargot*. Genes Dev. 8, 2270–2281.

Ghabrial, A., Luschnig, S., Metzstein, M.M., Krasnow, M.A., 2003. Branching morphogenesis of the *Drosophila* tracheal system. Annu. Rev. Cell Dev. Biol. 19, 623–647.

Goto, S., Hayashi, S., 1997. Specification of the embryonic limb primordium by graded activity of Decapentaplegic. Development 124, 125–132.

Graner, M.W., Bunch, T.A., Baumgartner, S., Kerschen, A., Brower, D.L., 1998. Splice variants of the *Drosophila* PS2 integrins differentially interact with RGD-containing fragments of the extracellular proteins tiggrin, ten-m, and D-laminin 2. J. Biol. Chem. 273, 18235–18241.

Guha, A., Kornberg, T.B., 2005. Tracheal branch repopulation precedes induction of the *Drosophila* dorsal air sac primordium. Dev. Biol. 287, 192–200.

Hayashi, S., Ito, K., Sado, Y., Taniguchi, M., Akimoto, A., Takeuchi, H., Aigaki, T., Matsuzaki, F., Nakagoshi, H., Tanimura, T., Ueda, R., Uemura, T., Yoshihara, M., Goto, S., 2002. GETDB, a database compiling expression patterns and molecular locations of a collection of Gal4 enhancer traps. Genesis 34, 58–61.

Henchcliffe, C., Garcia-Alonso, L., Tang, J., Goodman, C.S., 1993. Genetic analysis of laminin A reveals diverse functions during morphogenesis in *Drosophila*. Development 118, 325–337.

Hirano, S., Ui, K., Miyake, T., Uemura, T., Takeichi, M., 1991. *Drosophila* PS integrins recognize vertebrate vitronectin and function as cell–substratum adhesion receptors in vitro. Development 113, 1007–1016.

Hynes, R.O., 2002. Integrins: bidirectional, allosteric signaling machines. Cell 110, 673–687.

Isaac, D.D., Andrew, D.J., 1996. Tubulogenesis in *Drosophila*: a requirement for the *trachealess* gene product. Genes Dev. 10, 103–117.

Kassis, J.A., Noll, E., VanSickle, E.P., Odenwald, W.F., Perrimon, N., 1992. Altering the insertional specificity of a *Drosophila* transposable element. Proc. Natl. Acad. Sci. U. S. A. 89, 1919–1923.

Kato, K., Chihara, T., Hayashi, S., 2004. Hedgehog and Decapentaplegic instruct polarized growth of cell extensions in the *Drosophila* trachea. Development 131, 5253–5261.

Kiehart, D.P., Galbraith, C.G., Edwards, K.A., Rickoll, W.L., Montague, R.A., 2000. Multiple forces contribute to cell sheet morphogenesis for dorsal closure in *Drosophila*. J. Cell Biol. 149, 471–490.

Klambt, C., Glazer, L., Shilo, B.Z., 1992. *breathless*, a *Drosophila* FGF receptor homolog, is essential for migration of tracheal and specific midline glial cells. Genes Dev. 6, 1668–1678.

Kubota, K., Goto, S., Eto, K., Hayashi, S., 2000. EGF receptor attenuates Dpp signaling and helps to distinguish the wing and leg cell fates in *Drosophila*. Development 127, 3769–3776.

Kusche-Gullberg, M., Garrison, K., MacKrell, A.J., Fessler, L.I., Fessler, J.H., 1992. Laminin A chain: expression during *Drosophila* development and genomic sequence. EMBO J. 11, 4519–4527.

Llimargas, M., Casanova, J., 1999. EGF signalling regulates cell invagination as well as cell migration during formation of tracheal system in *Drosophila*. Dev. Genes Evol. 209, 174–179.

Luo, L., Liao, Y.J., Jan, L.Y., Jan, Y.N., 1994. Distinct morphogenetic functions of similar small GTPases: *Drosophila* Drac1 is involved in axonal outgrowth and myoblast fusion. Genes Dev. 8, 1787–1802.

Martin, D., Zusman, S., Li, X., Williams, E.L., Khare, N., DaRocha, S., Chiquet-Ehrismann, R., Baumgartner, S., 1999. *wing blister*, a new *Drosophila* laminin alpha chain required for cell adhesion and migration during embryonic and imaginal development. J. Cell Biol. 145, 191–201.

McDonald, K.L., 1994. Electron microscopy and EM immunocytochemistry. Methods Cell Biol. 44, 411–444.

Micklem, D.R., Dasgupta, R., Elliott, H., Gergely, F., Davidson, C., Brand, A., Gonzalez-Reyes, A., St Johnston, D., 1997. The mago nashi gene is required for the polarisation of the oocyte and the formation of perpendicular axes in *Drosophila*. Curr. Biol. 7, 468–478.

Miner, J.H., Li, C., Mudd, J.L., Go, G., Sutherland, A.E., 2004. Compositional and structural requirements for laminin and basement membranes during mouse embryo implantation and gastrulation. Development 131, 2247–2256.

Nermut, M.V., Green, N.M., Eason, P., Yamada, S.S., Yamada, K.M., 1988. Electron microscopy and structural model of human fibronectin receptor. EMBO J. 7, 4093–4099.

Ohshiro, T., Saigo, K., 1997. Transcriptional regulation of *breathless* FGF receptor gene by binding of TRACHEALESS/dARNT heterodimers to three central midline elements in *Drosophila* developing trachea. Development 124, 3975–3986.

Pastor-Pareja, J.C., Grawe, F., Martin-Blanco, E., Garcia-Bellido, A., 2004. Invasive cell behavior during *Drosophila* imaginal disc eversion is mediated by the JNK signaling cascade. Dev. Cell 7, 387–399.

Samakovlis, C., Hacohen, N., Manning, G., Sutherland, D.C., Guillemin, K., Krasnow, M.A., 1996. Development of the *Drosophila* tracheal system occurs by a series of morphologically distinct but genetically coupled branching events. Development 122, 1395–1407.

Sato, M., Kornberg, T.B., 2002. FGF is an essential mitogen and chemoattractant for the air sacs of the *Drosophila* tracheal system. Dev. Cell 3, 195–207.

Sepulveda, J.L., Gkretsi, V., Wu, C., 2005. Assembly and signaling of adhesion complexes. Curr. Top. Dev. Biol. 68, 183–225.

Shiga, Y., Tanaka-Matakatsu, M., Hayashi, S., 1996. A nuclear GFP beta-galactosidase fusion protein as a marker for morphogenesis in living *Drosophila*. Dev. Growth Differ. 38, 99–106.

Sutherland, D., Samakovlis, C., Krasnow, M.A., 1996. *branchless* encodes a *Drosophila* FGF homolog that controls tracheal cell migration and the pattern of branching. Cell 87, 1091–1101.

Tautz, D., Pfeifle, C., 1989. A non-radioactive in situ hybridization method for the localization of specific RNAs in *Drosophila* embryos reveals translational control of the segmentation gene *hunchback*. Chromosoma 98, 81–85.

Whitten, J., 1980. The tracheal system. In: Ashburner, M., Wright, T.R.F. (Eds.), The Genetics and Biology of *Drosophila*, vol. 2d. Academic Press Inc, London, pp. 499–539.

Wilk, R., Weizman, I., Shilo, B.Z., 1996. *trachealess* encodes a bHLH-PAS protein that is an inducer of tracheal cell fates in *Drosophila*. Genes Dev. 10, 93–102.